



Preparation of ultrafine silver powders with controllable size and morphology

Qing-hua TIAN^{1,2}, Duo DENG^{1,2}, Yu LI^{1,2}, Xue-yi GUO^{1,2}

1. School of Metallurgy and Environment, Central South University, Changsha 410083, China;

2. Cleaner Metallurgical Engineering Research Center, Nonferrous Metals Industry of China, Central South University, Changsha 410083, China

Received 2 June 2016; accepted 24 October 2017

Abstract: The ultrafine silver powders were prepared by liquid reduction method using Arabic gum as dispersant. The effects of different dispersants, pH values, and temperature on the morphology and particle size of silver powders were investigated. It is found that Arabic gum can better adsorb on silver particles via chemical adsorption, and it shows the best dispersive effect among all the selected dispersants. The particle size of silver powders can be finely tuned from 0.34 to 4.09 μm by adjusting pH values, while the morphology of silver powders can be tuned by changing the temperature. The silver powders with high tap density higher than 4.0 g/cm^3 were successfully prepared in a wide temperature range of 21.8–70 $^{\circ}\text{C}$. Especially, the tap density is higher than 5.0 g/cm^3 when the temperature is optimized to be 50 $^{\circ}\text{C}$. The facile process and high silver concentration of this method make it a promising way to prepare high quality silver powders for electronic paste.

Key words: ultrafine silver powder; Arabic gum; dispersion mechanism; tap density; controllable preparation

1 Introduction

Silver powders have been widely used in electronics [1], optical devices [2], antimicrobial [3] and catalysis [4] due to their unique electrical, optical, catalytic and thermal properties [5]. Silver electronic paste and silver thick paste, with silver powders as a major component, have been extensively used for electrical connection in silicon solar cells [6], hybrid circuits and other devices [7]. Physical features of silver powders, such as shape, size and tap density have great impact on the rheology of ink, and further the microstructure and the performance of the fired film [8,9]. Fine silver powders with good dispersity [10], proper particle size [11], and high tap density [12] are required for silver paste applied in high-end products such as front side metallization of crystalline silicon solar cell, plasma display panels(PDP), low temperature cofired ceramics(LTCC), etc.

Generally, micron silver powders have lower surface resistance, higher tap density and lower cost than nano silver powders when applied in silver paste. However, most researches focused on the preparation of

silver nanoparticles [13–15]. AJITHA et al [16] investigated the preparation of silver nanoparticles with particle size of 14–30 nm. YAN et al [17] investigated the capping effect of different reducing agents and surfactants in the synthesis of silver nanoplates. Researchers paid limited attention to the preparation of micron silver powders. Besides, little attention is paid to the synthesis of high-tap-density ($>4.0 \text{ g}/\text{cm}^3$) silver powders with controllable size and surface morphology. MOUDIR et al [18] synthesized micron silver powders in different alkaline solutions, but the prepared silver powders exhibit poor dispersity, and they paid no attention to the tap density and the size/shape controlling. What's more, the dispersion and growth mechanisms in preparing micron silver powders were rarely investigated. For instance, GU et al [19] synthesized silver powders with diameters of 0.2–2 μm using PVP as dispersant, but paid little attention to the dispersion and growth mechanism of silver powder. Thus, fabricating high-tap-density micron silver powders with controllable size and morphology, and investigating their formation and dispersion mechanism, are still a promising issue.

In this work, a simple liquid reduction route to prepare high-tap-density and micron-sized silver powders

Foundation item: Project (2014DFA90520) supported by the International Cooperation Program of Ministry of Science and Technology of China; Project (2013A090100003) supported by the Production, Teaching and Research Program of Guangdong Province, China; Project (2013DY048) supported by the Science and Technology Cooperation Program of Daye Nonferrous Metals Group, China

Corresponding author: Xue-yi GUO; Tel: +86-731-88877863; E-mail: xyguo@csu.edu.cn
DOI: 10.1016/S1003-6326(18)64685-0

with controllable size and morphology was studied. The effects of different dispersants, pH values and temperature on particle size and morphology of silver powders were investigated. The dispersion mechanism of different dispersants was investigated, and the growth mechanism of the silver powders was studied. The results demonstrated that Arabic gum can be adsorbed on the surface of the silver particles well via chemical adsorption, and it shows a better dispersive effect than other dispersants. The particle size (0.34–4.09 μm) and crystallite size can be finely tuned by adjusting pH value and temperature, the tap density ($>4.0 \text{ g/cm}^3$) and particle surface morphology are also tunable. The facile process and high silver concentration of this method are of two advantages that contribute to the large-scale production of high-quality silver powders, which can be applied in plasma display panels (PDP), low temperature cofired ceramics (LTCC), multilayer ceramic capacitor (MLCC), and solar cell.

2 Experimental

2.1 Chemicals

Analytical reagents of silver nitrate (AgNO_3), ascorbic acid ($\text{C}_6\text{H}_8\text{O}_6$), tween-80 (TW-80), and polyvinyl alcohol-124 (PVA-124) were purchased from Xilong Chemical Co., Ltd., China. Analytical reagents of Arabic gum (AG), polyethylene glycol-10000 (PEG-10000), polyvinyl pyrrolidone-K30 (PVP-K30), and aqueous ammonia ($\text{NH}_3\cdot\text{H}_2\text{O}$, 25%–28%) were purchased from Sinopharm Chemical Reagent Co., Ltd., China. All the reagents were used without further purification.

2.2 Preparation of silver powders

In a typical experiment, 200 mL aqueous solution containing 25 g AgNO_3 was added into 1250 mL aqueous solution containing 25 g ascorbic acid and 3 g AG (dispersant dosage is 12% relative to AgNO_3 mass) with feeding rate of 1.1 mL/s under vigorous agitation of 300 r/min at a constant temperature of 50 °C. The pH value of ascorbic acid solution was adjusted by aqueous ammonia. The as-prepared silver powders were separated from the solution by centrifugation and washed with deionized water and anhydrous ethanol three times, respectively. Subsequently, they were dried at 50 °C in a vacuum oven for 10 h.

2.3 Characterization

The morphology and size of the prepared silver powders were investigated by scanning electron microscopy (SEM) with a JSM-6360LV instrument while their crystalline structure was determined by X-ray diffraction (XRD) using a Rigaku-TTR III diffractometer

using the $\text{Cu K}\alpha$ as radiation with a wavelength of 1.5406 Å. The UV–Vis spectra of aqueous solutions were measured by UV–Vis spectrophotometer (Hitachi U-4100). The FTIR spectra of silver powders and AG were measured by FTIR spectrometer (Nicolet 6700). The tap density of silver powders was determined by a particle density tester (ZS-202).

3 Results and discussion

3.1 Effect of dispersant

The effect of dispersants (AG, TW-80, PEG-10000, PVP-K30, and PVA-124) on the morphology of silver powders was investigated and shown in Fig. 1. In Fig. 1(a), the silver powder prepared with AG is quasi-spherical and well-dispersed, with an average particle size of 2–3 μm , while the silver powders prepared with other dispersants show serious agglomeration. The silver powders prepared with PEG-10000 (Fig. 1(c)) and PVA-124 (Fig. 1(e)) as dispersants exhibit tree-like structure, composed of dendrite branches, with average size of 3–10 μm . While the silver powders prepared with TW-80 (Fig. 1(b)) and PVP-K30 (Fig. 1(d)) as dispersants are of flower-like structure, which are constructed by several smaller silver particles. It is obvious that silver powders prepared with AG as dispersant show better dispersity than the others. Figure 2 shows the XRD patterns of silver powders prepared with different dispersants, and all the diffraction peaks observed in the spectra can be indexed to (111), (200), (220) and (311) crystal planes of silver with a face-centered cubic (FCC) phase structure, which indicate that they are metallic silver, and no silver oxide or residue is detected, implying that the use of different dispersants didn't influence the composition of silver powders. The diffraction peaks of these samples are all sharp (although have different intensities), indicating that these silver powders have high crystallinity.

The UV–Vis spectra of AgNO_3 solution with/without dispersants were tested and shown in Fig. 3. The AgNO_3 solution has an absorption peak at 300 nm (with absorption intensity of 0.235), due to the coordinative bonds of $\text{H}_2\text{O}:\text{Ag}^+:\text{OH}_2$ in UV spectra [20,21]. The AgNO_3 solutions with dispersants of PVP-K30, AG, PVA-124 and TW-80 added show stronger UV absorption peaks at 300 nm (with absorption intensities of 0.264, 0.366, 0.263 and 0.308, respectively) than the pure AgNO_3 solution. The larger absorption intensity after introducing dispersants may be attributed to the complex formed by Ag^+ and dispersants. This is because Ag^+ has two empty sp hybrid orbitals, whereas PVP-K30, AG, PVA-124, and TW-80 have many C—N, —OH or C=O groups, which contributed more electronic density to the sp orbital of Ag^+ than H_2O

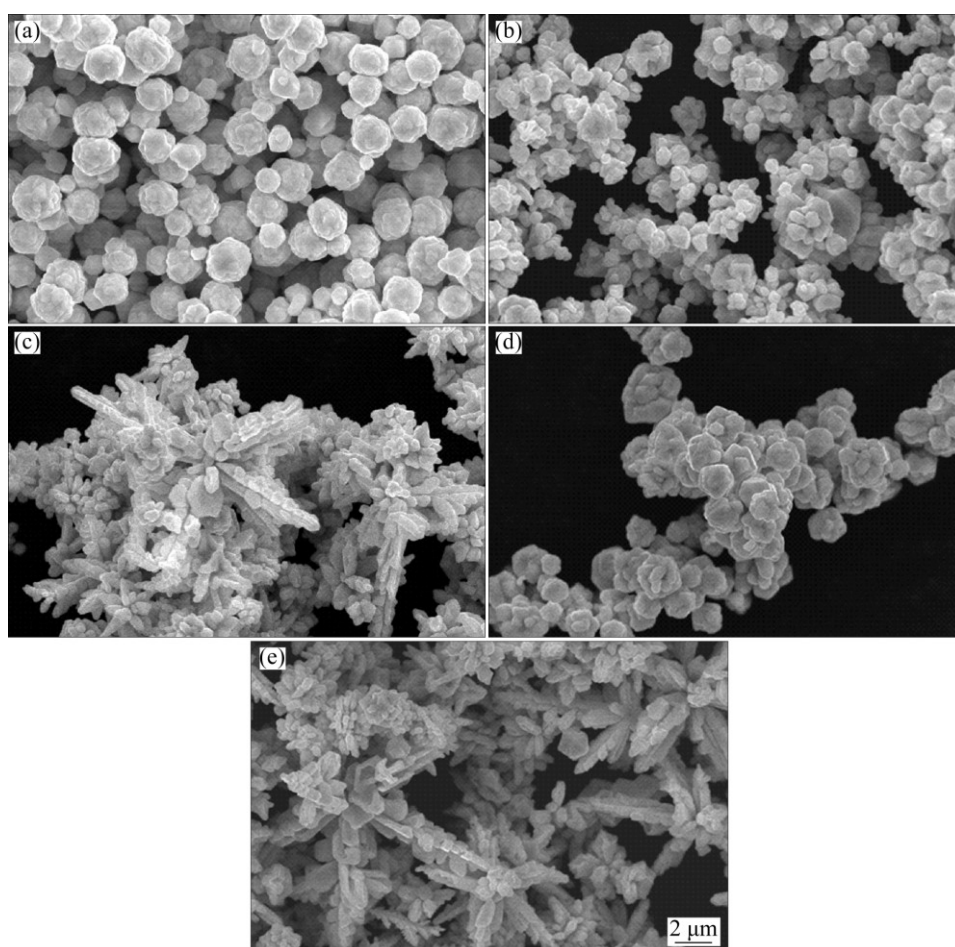


Fig. 1 SEM images of silver powders prepared with different dispersants: (a) AG; (b) TW-80; (c) PEG-10000; (d) PVP-K30; (e) PVA-124

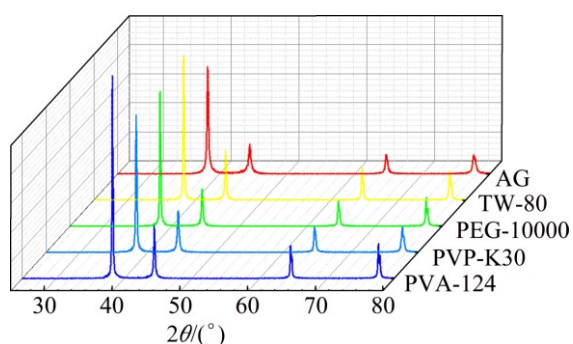


Fig. 2 XRD patterns of silver powders prepared with different dispersants

did [22]. The more electronic density the dispersants contributed to the sp orbital of Ag^+ , the stronger Ag^+ coordination ability the dispersants have. These lead to the stronger absorption at 300 nm in UV spectra. Hence, it can be inferred from Fig. 3 that AG has the strongest coordination ability with Ag^+ compared with other dispersants. On the contrary, the addition of PEG-10000 has no obvious impact on the absorption intensity of $AgNO_3$ solution (with absorption intensity of 0.230 at 300 nm), implying its weak Ag^+ coordination ability.

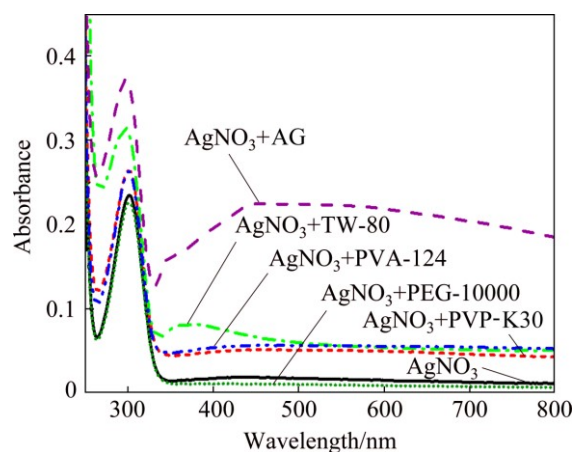


Fig. 3 UV-Vis absorption spectra of $AgNO_3$ solution and $AgNO_3$ solution with different dispersants

In Fig. 3, it is also found that the UV spectrum of $AgNO_3+AG$ solution shows an obvious absorption band around 470 nm, indicating the formation of silver nanoparticles. This may be because AG can contribute more electronic density to the sp orbital of Ag^+ and reduce Ag^+ to silver particles. Therefore, AG plays an

important role in promoting the nucleation of the metallic silver particles and facilitating the photo-reduction of Ag^+ .

As Ag still has a vacant orbital, silver particles tend to attract electron-donating group, previous research also found that PVP molecules can loan pair electrons to silver [21]. Thus, the stronger electron donating ability of AG makes it easier to adsorb on the surface of the silver particles than other dispersants, leading to higher covering fraction of AG on silver particles, thus ensuring better dispersion effect of AG. The adsorption of AG on silver powders can be confirmed by the FTIR spectra shown in Fig. 4. It is obvious that the silver powders exhibit similar spectrum with AG even they have been washed many times, suggesting that there are some AG residues on the silver powders due to their strong adsorption ability on the surface of silver powders. Compared with the FTIR spectrum of AG, the $\text{C}=\text{O}$ absorption peak of silver powders at 1424 cm^{-1} is weak, while the $\text{C}=\text{O}$ absorption peak at 1645 cm^{-1} shifts to 1627 cm^{-1} , indicating that AG may coordinate with silver particles by $\text{C}=\text{O}$ group and help to stabilize the silver particles [23]. Furthermore, the $\text{C}-\text{O}$ absorption

peak of silver powders at 1072 cm^{-1} is shifted to 1076 cm^{-1} , while the $\text{C}-\text{H}$ absorption peak at 2931 cm^{-1} is divided into two peaks of 2854 and 2922 cm^{-1} , and the $-\text{OH}$ absorption peak at 3421 cm^{-1} is shifted to 3439 cm^{-1} . The shifts and division of these absorption peaks imply that the adsorption between AG and silver powder is chemical adsorption, but not simple physical adsorption.

AG molecule has a 150 nm long chain [24] and possesses highly branched structure, and the main chain of AG consists of 1,3-linked-*D*-galactopyranosyl units while side chains are composed of 1,3-linked-*D*-galactopyranosyl, *L*-arabinofuranosyl, *L*-rhamnopyranosyl and *D*-glucopyranosyl uronic acid units [25,26]. When AgNO_3 solution is added into the ascorbic acid solution, Ag^+ is reduced into silver atoms and the atoms start to nucleate and then grow to form primary particles. With continual adding of AgNO_3 , more and more Ag^+ ions are reduced and more primary particles are generated. The primary particles would further grow into secondary particles by the aggregation growth. As AG can be adsorbed on the surface of the silver particles, the highly branched long chain structure of AG molecules can provide good steric restriction, which prevents silver particles from agglomerating and the as-formed secondary particles from further growing. As a result, the silver particles are well dispersed and the particle size can be controlled. The detailed dispersion mechanism of AG is illustrated in Fig. 5.

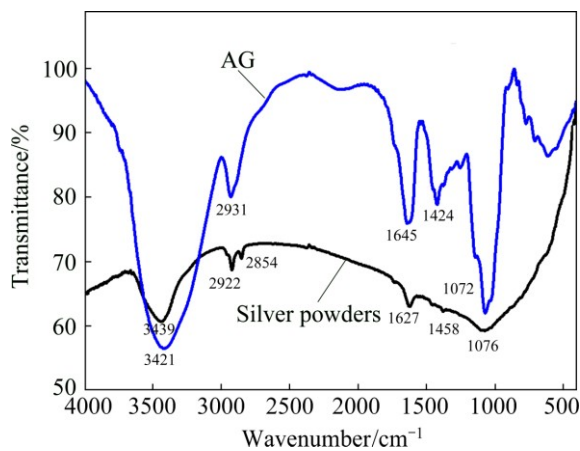


Fig. 4 FTIR spectra of AG and silver powders prepared with AG as dispersant

3.2 Effect of pH values

The effect of pH values on particle size and morphology of silver powders was investigated. By adding different amounts of aqueous ammonia, the pH values of ascorbic acid solution were adjusted to 2.73, 4.24, 6.13, 9.20 and 9.46, respectively. The SEM images of silver powders prepared at different pH values are shown in Fig. 6. It is obvious that the diameter of silver powders decreases rapidly with increasing pH value. The

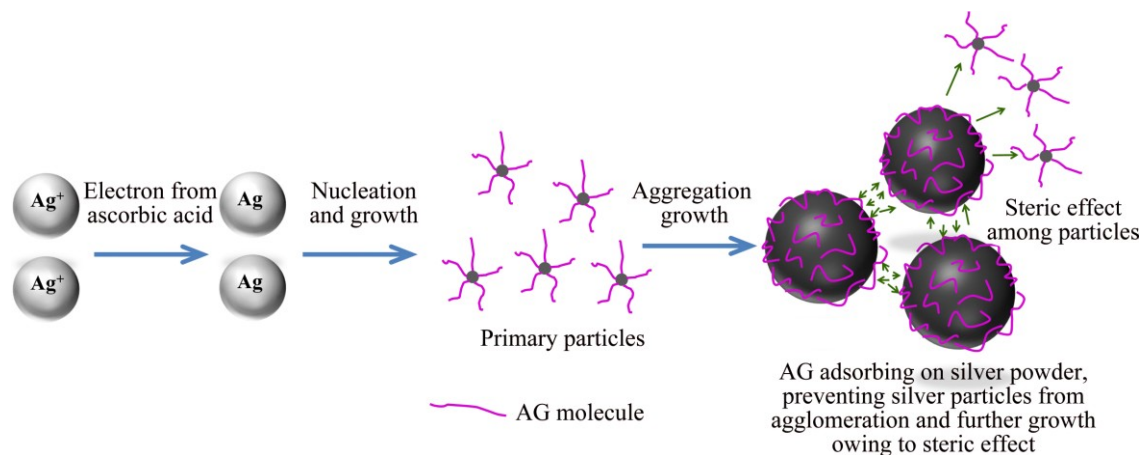


Fig. 5 Dispersion mechanism of AG in preparation of silver powders

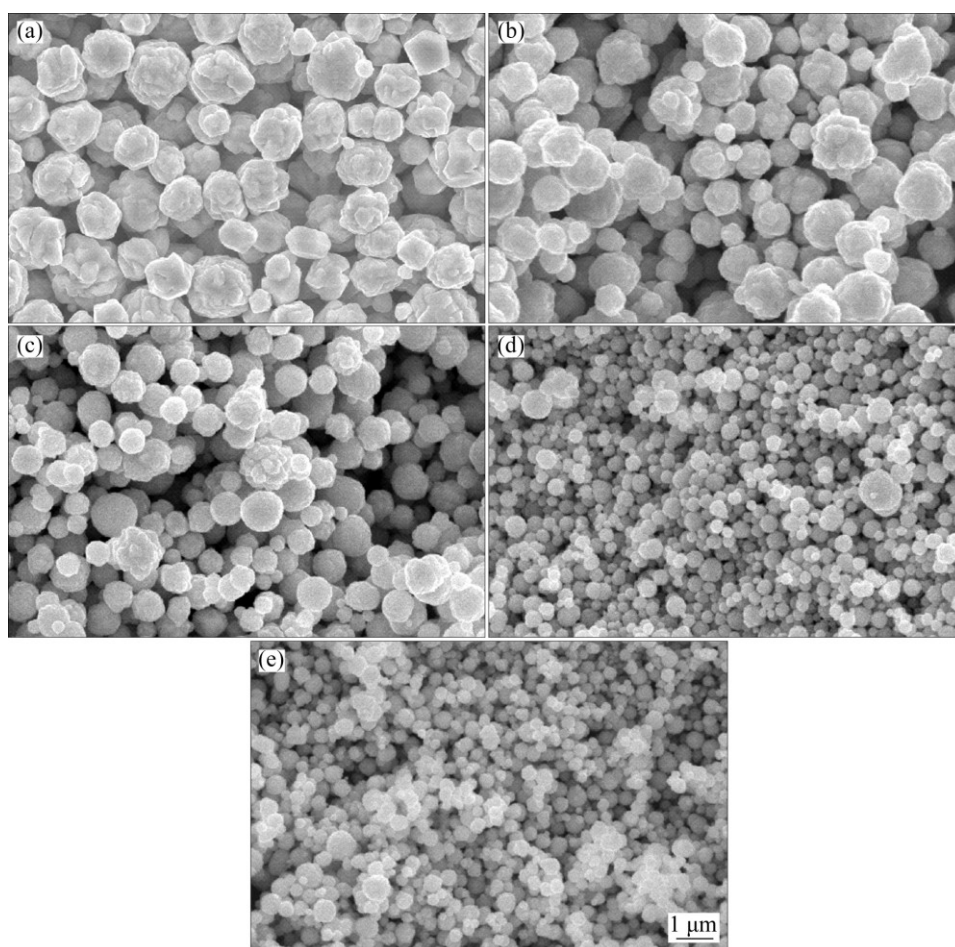


Fig. 6 SEM images of silver powders prepared at different pH values: (a) pH=2.73; (b) pH=4.24; (c) pH=6.13; (d) pH=9.20; (e) pH=9.46

silver powders are quasi-spherical with rough surface when the pH value is 2.73. As the pH value increases, the shape of silver powders becomes more regular and their surface becomes smoother. Figure 7 shows the distribution and variation of the silver particle size. It is obviously observed that the particle size decreases from 2.60 to 0.34 μm as the pH value increases from 2.73 to 9.46. Meanwhile, the size distribution becomes narrow.

Ascorbic acid is a kind of weak acid, and it has excellent reduction ability [27]. The electrode reaction equation is



According to the Nernst equation, the electrode potential of ascorbic acid can be expressed as follows:

$$\varphi = \varphi^\ominus - 0.0591\text{pH} \quad (2)$$

It is easy to conclude that the reducing power of ascorbic acid can be tuned by changing the pH value. As the pH value increases, the reducing power of ascorbic acid increases, and the reducing rate of the reduction of Ag^+ rises. The faster reducing rate would

result in the faster nucleation rate, thus leading to the formation of more nuclei and the decrease of the silver particle size. Therefore, the particle size of silver powders can be tuned by simply changing the pH value of ascorbic acid.

The higher pH value also leads to the decrease of crystallite size (estimated by the Scherrer's equation, as shown in Fig. 7(f)). These crystallites are the subunits of silver particles. The silver particles are formed by aggregation growth of the subunits [28]. The decreased crystallite size can be responsible for the smoother surface of silver particle as the pH value increases. Besides, HALACIUGA and GOIA [10] found that the appearance of surface was likely determined by the dynamics of rearrangement of nano-sized subunits during the aggregation process. The slower rearrangement of subunits would lead to the formation of more rough surfaces, while more rapid rearrangements lead to the formation of smoother surface. In this study, the reaction rate is faster at higher pH value, so the rearrangement of subunits is faster and the surface of silver particles is smoother.

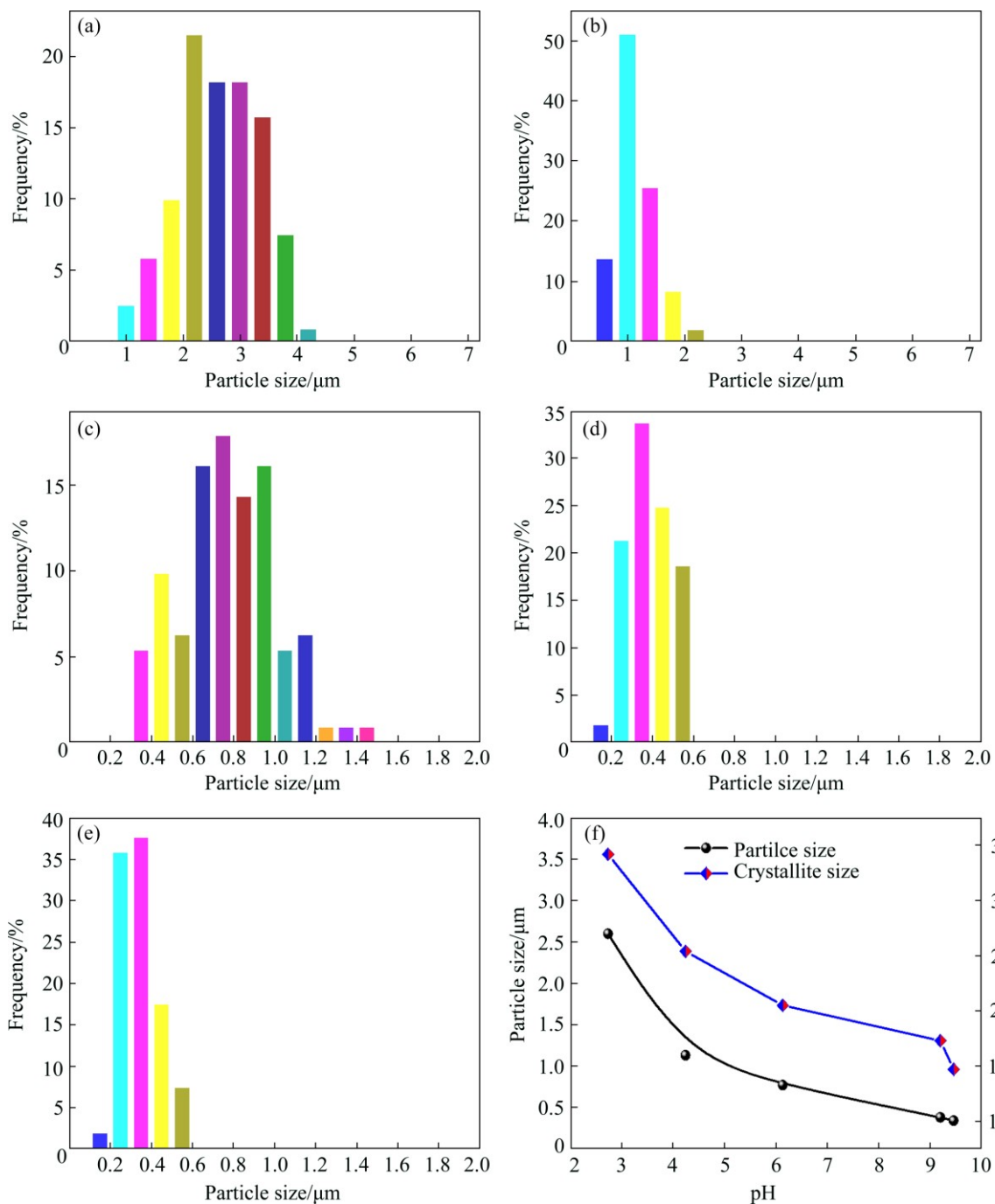


Fig. 7 Size distributions of silver powders prepared at different pH values of pH=2.73 (a), pH=4.24 (b), pH=6.13 (c), pH=9.20 (d), pH=9.46 (e) and variation of silver particle size and crystallite size with pH value (f)

3.3 Effect of temperature

The effect of temperature on particle size and morphology of silver powders was investigated. The temperature was set at 21.8 (room temperature), 30, 40, 50, 60 and 70 °C, respectively. Figure 8 shows the SEM images of silver powders prepared at different temperatures. Silver powders are in quasi-spherical shape with good dispersity in the range 21.8–70 °C, and the silver particle size decreases as the temperature increases. The variation of particle size at different

temperatures is shown in Fig. 9. It is found that the particle size is 4.09 μm at 21.8 °C, and decreases to 2.51 μm at 70 °C, which is attributed to the faster nucleation rate at higher temperature [29]. Hence, the silver particle size can also be tuned by adjusting the temperature.

Besides, the surface of silver particles becomes smoother as the temperature increases. Figure 10 shows the high magnification SEM images of silver particles prepared at different temperatures. The surfaces of

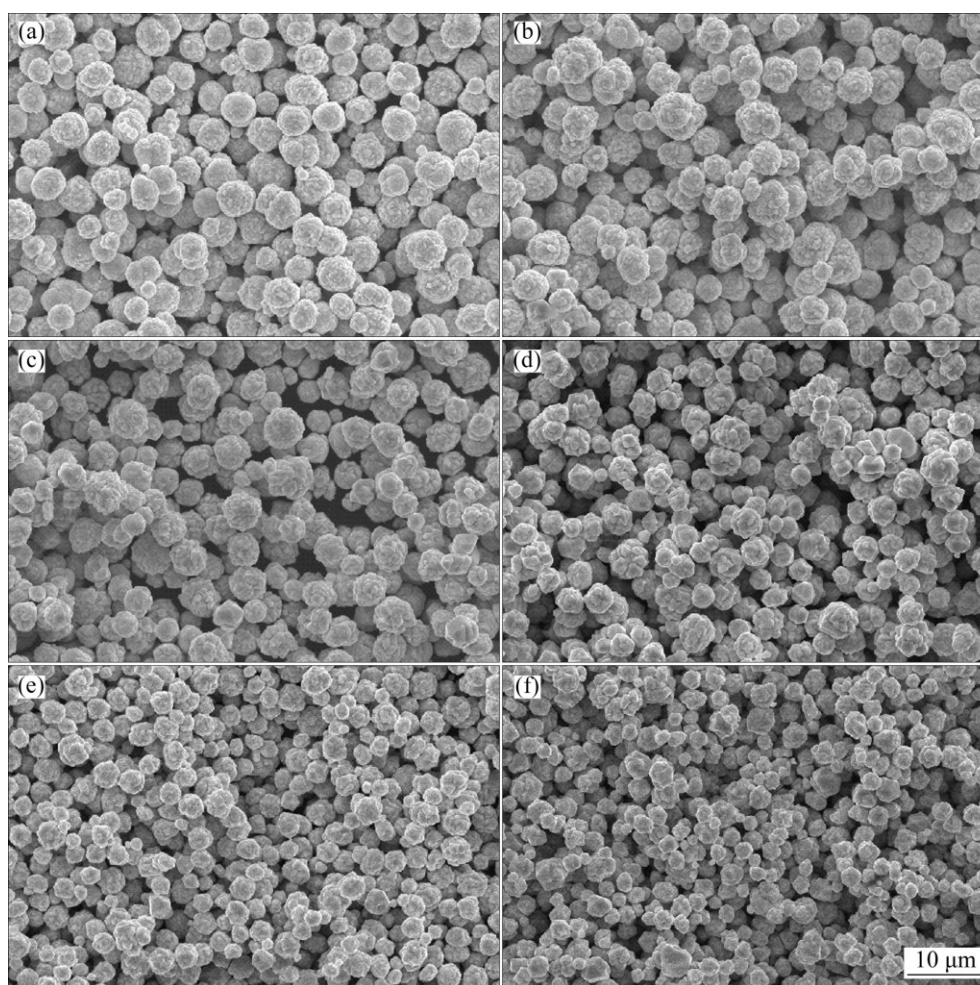


Fig. 8 SEM images of silver powders prepared at different temperatures: (a) 21.8 °C; (b) 30 °C; (c) 40 °C; (d) 50 °C; (e) 60 °C; (f) 70 °C

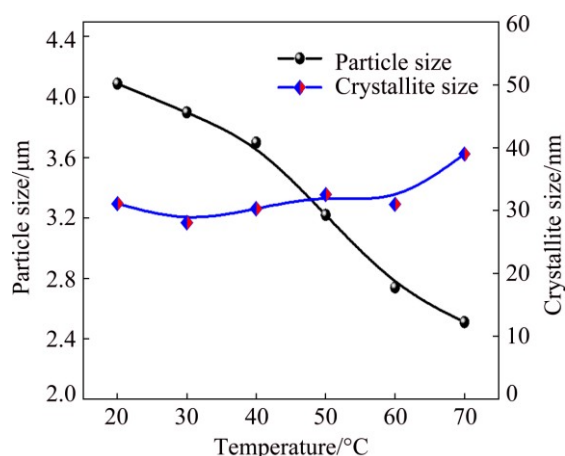


Fig. 9 Variation of particle size and crystallite size of silver powders at different temperatures

silver particles are very rough at 21.8–40 °C, which are composed of many primary particles, indicating that they are formed by the aggregation growth of these primary particles (in accordance with Fig. 5). With increasing the temperature, their surfaces become smoother, and their

shapes are transformed from quasi-spherical to polyhedral.

As the crystallite size increases slightly with the increase of temperature (Fig. 9), the morphology of surface is most likely determined by the dynamics of rearrangement of nano-sized subunits. The rearrangement of subunits appears to be slow at low temperature, which results in a rough surface at 21.8–40 °C, and it is faster at higher temperature, leading to the formation of smoother surface.

The tap density was measured and the results are listed in Table 1. The tap density of silver powders prepared at 21.8–70 °C is higher than 4.0 g/cm³. From Table 1, it is obvious that the tap density increases with the increase of temperature (21.8–50 °C), while the

Table 1 Tap density of silver powders prepared at different temperatures

Temperature/°C	21.8	30	40	50	60	70
Tap density/(g·cm ⁻³)	4.14	4.62	4.81	5.17	4.88	5.02

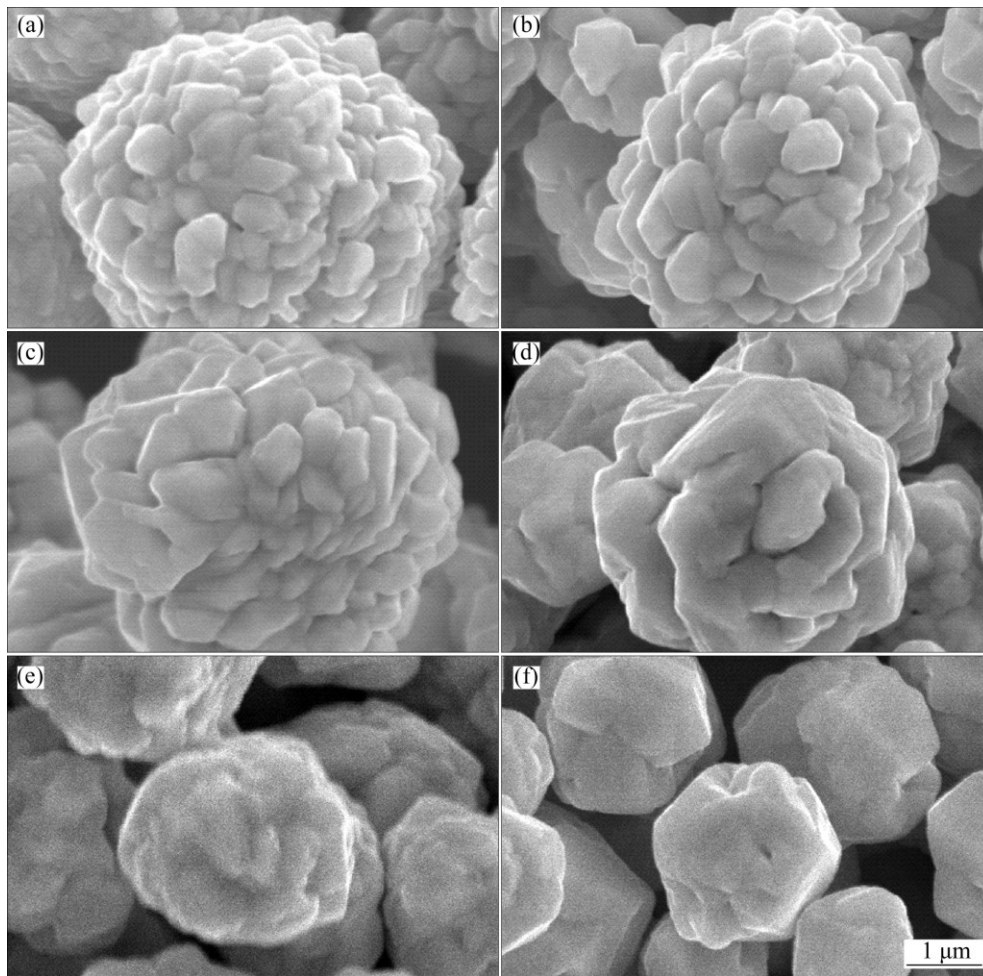


Fig. 10 High magnification SEM images of silver particles prepared at different temperatures: (a) 21.8 °C; (b) 30 °C; (c) 40 °C; (d) 50 °C; (e) 60 °C; (f) 70 °C

particle size decreases with the increase of temperature (as shown as Fig. 9). This may be due to different roughness values among these silver powders. Roughness influences the sliding friction between particles, and powders with rougher surface have larger sliding friction, which would prevent them from packing densely [30]. As shown in Fig. 10, it is clear that the silver powders prepared at higher temperature have a smoother surface, so the sliding friction between silver particles decreases, which leads to the increase of tap density. The tap density then decreases with the continual increase of temperature (50–70 °C), which is ascribed to the decrease of silver particle size.

4 Conclusions

1) Micron-sized silver powders with high tap density ($>4 \text{ g/cm}^3$) and good dispersity were prepared with AG as dispersant.

2) Silver powders prepared with PEG-10000 and PVA-124 as dispersants exhibit tree-like structure. Silver

powders prepared with TW-80 and PVP-K30 exhibit flower-like structure. While silver powders prepared with AG as dispersant are quasi-spherical and show the best dispersity. The study on the mechanism shows that AG molecules can be adsorbed on the surface of silver particles well via chemical adsorption, thus ensuring good dispersity of the silver particles.

3) As pH value increases from 2.73 to 9.46, the silver particle size can be finely tuned from 4.09 to 0.34 μm . The crystallite size, tap density, and the surface morphology of silver powders can also be tuned by changing the pH value and temperature.

References

- [1] LI Wei, WU Tao, JIAO Ruo-bing, ZHANG Bo-ping, LI Si-yang, ZHOU Yang, LI Liang-liang. Effects of silver nanoparticles on the firing behavior of silver paste on crystalline silicon solar cells [J]. *Colloids and Surfaces A: Physicochemical and Engineering Aspects*, 2015, 466: 132–137.
- [2] LUO Sui-lian, CHEN Yao, FAN Guang-hua, SUN Feng-qiang, QU Shi-liang. Saturable absorption and reverse saturable absorption on

- silver particles with different shapes [J]. *Applied Physics A*, 2014, 117: 891–894.
- [3] CHENG F, BETTS J W, KELLY S M, HECTOR A L. Green synthesis of highly concentrated aqueous colloidal solutions of large starch-stabilised silver nanoplatelets [J]. *Materials Science and Engineering C*, 2015, 46: 530–537.
- [4] SAGITHA P, SARADA K, MURALEEDHARAN K. One-pot synthesis of poly vinyl alcohol (PVA) supported silver nanoparticles and its efficiency in catalytic reduction of methylene blue [J]. *Transactions of Nonferrous Metals Society of China*, 2016, 26: 2693–2700.
- [5] GUO Xue-yi, DENG Duo, TIAN Qing-hua, JIAO Cui-yan. One-step synthesis of micro-sized hexagon silver sheets by the ascorbic acid reduction with the presence of H_2SO_4 [J]. *Advanced Powder Technology*, 2014, 25: 865–870.
- [6] ZHAI Ai-xia, CAI Xiong-hui, DU Bin. A novel wet-chemical method for preparation of silver flakes [J]. *Transactions of Nonferrous Metals Society of China*, 2014, 24: 1452–1457.
- [7] IRIZARRY R, BURWELL L, LEÓN-VELÁZQUEZ M S. Preparation and formation mechanism of silver particles with spherical open structures [J]. *Industrial & Engineering Chemistry Research*, 2011, 50: 8023–8033.
- [8] HILALI M M, NAKAYASHIKI K, KHADILKAR C, REEDY R C, ROHATGI A, SHAIKH A, KIM S, SRIDHARAN S. Effect of Ag particle size in thick-film Ag paste on the electrical and physical properties of screen printed contacts and silicon solar cells [J]. *Journal of the Electrochemical Society A*, 2006, 153: 5–11.
- [9] LI Rui-xiao, TAI Yu-ping, BAI Jin-tao, WANG Hui. Effect of spherical silver powders with different sizes in back electrode paste on the conversion efficiency of silicon solar cells [J]. *Journal of Materials Science: Materials in Electronics*, 2015, 26: 2471–2479.
- [10] HALACIUGA I, GOIA D V. Preparation of silver spheres by aggregation of nanosize subunits [J]. *Journal of Materials Research*, 2008, 23: 1776–1784.
- [11] WANG Hai-ying, TAI Yu-ping, LI Rui-xiao, WANG Hui, BAI Jin-tao. Effect of the mass ratio of micron and submicron silver powder in the front electrode paste on the electrical performance of crystalline silicon solar cells [J]. *Royal Society of Chemistry*, 2016, 6: 28289–28297.
- [12] WANG Gang, BAI Jin-tao, WANG Hui, CUI Yan-bin. Preparation of micro-sized and monodisperse crystalline silver particles used for silicon solar cell electronic paste [J]. *Journal of Materials Science: Materials in Electronics*, 2014, 25: 487–494.
- [13] ZHANG Lei, WANG Yi, TONG Li-min, XIA You-nan. Seed-mediated synthesis of silver nanocrystals with controlled sizes and shapes in droplet microreactors separated by air [J]. *Langmuir*, 2013, 29: 15719–15725.
- [14] YANG Zhi-lin, ZHAI Dan-dan, WANG Xiao, WEI Jie. In situ synthesis of highly monodispersed nonaqueous small-sized silver nano-colloids and silver/polymer nanocomposites by ultraviolet photopolymerization [J]. *Colloids and Surfaces A: Physicochemical and Engineering Aspects*, 2014, 448: 107–114.
- [15] LI Ying-fen, GAN Wei-ping, ZHOU Jian, LU Zhi-qiang, YANG Chao, GE Tian-tian. Hydrothermal synthesis of silver nanoparticles in Arabic gum aqueous solutions [J]. *Transactions of Nonferrous Metals Society of China*, 2015, 25: 2081–2086.
- [16] AJITHA B, ASHOK KUMAR REDDY Y, SREEDHARA REDDY P. Enhanced antimicrobial activity of silver nanoparticles with controlled particle size by pH variation [J]. *Powder Technology*, 2015, 269: 110–117.
- [17] YAN Yang, CHEN Ke-bin, LI Hao-ran, HONG Wei, HU Xiao-bin, XU Zhou. Capping effect of reducing agents and surfactants in synthesizing silver nanoplates [J]. *Transactions of Nonferrous Metals Society of China*, 2014, 24: 3732–3738.
- [18] MOUDIR N, BOUKENOUS Y, MOULAI-MOSTEFA N, BOZETINE I, MAOUDJ M, KAMEL N, KAMEL Z, MOUDIR D. Preparation of silver powder used for solar cell paste by reduction process [J]. *Energy Procedia*, 2013, 36: 1184–1191.
- [19] GU Sa-sa, WANG Wei, WANG Hui, TAN Fa-tang, QIAO Xue-liang, CHEN Jian-guo. Effect of aqueous ammonia addition on the morphology and size of silver particles reduced by ascorbic acid [J]. *Powder Technology*, 2013, 233: 91–95.
- [20] GUO Gui-quan, GAN Wei-ping, LUO Jian, XIANG Feng, ZHANG Jin-ling, ZHOU Hua, LIU Huan. Preparation and dispersive mechanism of highly dispersive ultrafine silver powder [J]. *Applied Surface Science*, 2010, 256: 6683–6687.
- [21] ZHANG Zong-tao, ZHAO Bin, HU Li-ming. PVP protective mechanism of ultrafine silver powder synthesized by chemical reduction processes [J]. *Journal of Solid State Chemistry*, 1996, 121: 105–110.
- [22] AO Yi-wei, YANG Yun-xia, YUAN Shuang-long, DING Li-hua, CHEN Guo-rong. Preparation of spherical silver particles for solar cell electronic paste with gelatin protection [J]. *Materials Chemistry and Physics*, 2007, 104: 158–161.
- [23] KUMAR B, SMITA K, DEBUT A, CUMBAL L. Extracellular green synthesis of silver nanoparticles using Amazonian fruit Araza (*Eugenia stipitata* McVaugh) [J]. *Transactions of Nonferrous Metals Society of China*, 2016, 26: 2363–2371.
- [24] LI Ying-fen, GAN Wei-ping, LIU Xiao-gang, LIN Tao, HUANG Bei. Dispersion mechanisms of Arabic gum in the preparation of ultrafine silver powder [J]. *Korean Journal of Chemical Engineering*, 2014, 31: 1490–1495.
- [25] ALI B H, ZIADA A, BLUNDEN G. Biological effects of gum arabic: A review of some recent research [J]. *Food Chem Toxicol*, 2009, 47: 1–8.
- [26] GILS P S, RAY D, SAHOO P K. Designing of silver nanoparticles in gum arabic based semi-IPN hydrogel [J]. *International Journal of Biological Macromolecules*, 2010, 46: 237–244.
- [27] LIU Zhao, QI Xue-liang, WANG Hui. Synthesis and characterization of spherical and mono-disperse micro-silver powder used for silicon solar cell electronic paste [J]. *Advanced Powder Technology*, 2012, 23: 250–255.
- [28] GOIA D V. Preparation and formation mechanisms of uniform metallic particles in homogeneous solutions [J]. *Journal of Materials Chemistry*, 2004, 14: 451–458.
- [29] PARK J, PRIVMAN V, MATIJEVIĆ E. Model of formation of monodispersed colloids [J]. *The Journal of Physical Chemistry B*, 2001, 105: 11630–11635.
- [30] OUYANG Hong-wu, LIU Yong, WANG Hai-bin, HUANG Bai-yun. Calculation method for random packing of sphere particles [J]. *Materials Science and Engineering of Powder Metallurgy*, 2002, 7: 87–92. (in Chinese)

具有可控粒径和形貌超细银粉的合成

田庆华^{1,2}, 邓多^{1,2}, 李宇^{1,2}, 郭学益^{1,2}

1. 中南大学 冶金与环境学院, 长沙 410083;

2. 中南大学 中国有色金属工业协会清洁冶金工程研究中心, 长沙 410083

摘要: 以阿拉伯树胶为分散剂, 采用液相还原法制备超细银粉。探讨分散剂种类、pH 值和温度对银粉形貌和粒径的影响。研究表明, 阿拉伯树胶通过化学吸附作用可以更好地吸附在银粒子表面, 且比其他分散剂具有更好的分散作用。通过调节 pH 值, 银粉的粒径可在 0.34~4.09 μm 的范围内调节; 通过改变反应温度可以控制银粉的表面形貌。在 21.8~70 $^{\circ}\text{C}$ 的温度范围内, 可成功制备振实密度大于 4.0 g/cm^3 的银粉。在 50 $^{\circ}\text{C}$ 的最优温度下, 银粉的振实密度大于 5.0 g/cm^3 。该合成方法具有条件温和、银浓度高的优点, 是一种合成用于电子浆料的高品质银粉的有前景的方法。

关键词: 超细银粉; 阿拉伯树胶; 分散机理; 振实密度; 可控制备

(Edited by Wei-ping CHEN)